OPTICS, LASERS, AND QUANTUM ELECTRONICS

VALENCE BAND STRUCTURE, OPTICAL TRANSITIONS, AND LIGHT GAIN SPECTRUM IN PSEUDOMORPHICALLY STRAINED ZINC-BLENDE GaN QUANTUM WELLS

L.O. LOKOT

V.E. Lashkarev Institute of Semiconductor Physics, Department of Theoretical Physics, Nat. Acad. of Sci. of Ukraine

(41, Nauky Ave., Kyiv 03028, Ukraine; e-mail: llokot@gmail.com)

The influence of strains on the valence band spectrum, the interband matrix elements, and the light gain spectrum in zinc-blende GaN quantum wells has been studied. In the framework of the effective mass theory, the Schrödinger equation with a 3×3-block Hamiltonian was solved for the valence band. The results are illustrated for a $GaN/Al_{0.14}Ga_{0.86}N$ quantum well. It was found that, provided a biaxial compressive strain, the matrix elements of optical transitions from the heavy-hole subband correspond to a strict polarization of light in the quantum well plane. The large negative mass and the strong modification of the momentum matrix elements were connected to a biaxial tensile strain effects. The "random" double degeneration of spin-degenerate heavy- and light-hole states at the center of the Brillouin zone was found. The matrix element for the polarization in the direction perpendicular to the quantum well plane was found to be large. The biaxial strain was demonstrated to cause quite significant changes in the gain spectra of heterostructures. The tensile strain and the appearance of a circular loop of valence band maxima in the heterostructure were shown to be accompanied by a suppression of the laser effect. At the same time, the stimulated optical transitions are well pronounced at a compressive strain. Our results testify that internal strain effects are important for studying the optical properties of GaN and corresponding heterostructures.

1. Introduction

Direct wide-band-gap nitride semiconductors of group III, which are based on GaN, are intensively studied owing to their application in optoelectronic devices, such as light diodes and lasers in the green, blue, and ultra-violet spectral ranges, as well as ultra-violet photodetectors [1, 2]. Ultra-violet light-emitting diodes [3–8] and laser diodes [9–15] have already found their application. However, nitride structures and devices on their basis are only at the research stage.

Internal strain effects in heterostructures are important for modern semiconductor technology. They arise, in particular, when GaN is grown up on Si, SiC, GaAs, ZnO, and sapphire crystalline substrates. Internal deformations are connected with a large mismatch between crystal lattices and with the difference between the coefficients of temperature expansion of the epitaxial layer and the substrate. They can induce large biaxial strains in the epitaxial layer. There can be compressive or tensile biaxial strains, depending on the crystalline substrate material [16–18]. In this article, the effects of internal deformations are studied. We report the results of our researches dealing with the influence of a biaxial strain on the valence band structure of the quantum well GaN/AlGaN with the zinc blende type lattice and the width w which is oriented perpendicular to the growth direction (001) and localized in the spatial region $-w/2 < z < w/2$. The transverse components of the biaxial strain are proportional to the difference a_0 between the lattice constants and also depend on the Al content, x: $\epsilon_{xx} = \epsilon_{yy} = x\,(a_0^{AlN} - a_0^{GaN})/a_0^{GaN} = -0.029x < 0$, whereas $\epsilon_{xy} = \epsilon_{yz} = \epsilon_{xz} = 0$ [19]. The longitudinal component can be expressed as $\epsilon_{zz} = -2(C_{12}/C_{11})\,\epsilon_{xx}$, where C_{12} and C_{11} are the elastic constants. Since $\epsilon_{xx} < 0$, the lattice mismatch gives rise to a biaxial compressive deformation of the quantum well. In this paper, the situation where the crystalline substrate is the origin of tensile strains in the quantum well is also analyzed. To compare the roles played by compressive and tensile biaxial strain effects, we also consider an undeformed GaN thin film.

Our research does not consider polarization effects which are very important in such structures.

In order to describe the light emission and absorption processes, we calculated the energy, as well as the wave functions of the lowest conduction band and the valence subbands. We found the dependences of matrix elements of the dipole optical interband transition and the light gain spectrum in the zinc-blende GaN quantum well on the deformation.

The point group of a structure with a zinc blende type lattice is identical to elements of the tetrahedron point group which is denoted as T_d. The space group of such a structure is symmorphic, being denoted as T_d^2 [20]. Bonds between the closest neighbors in a wurtzite crystal also form a tetrahedron. The configuration of the closest neighbors within the first coordination sphere of the wurtzite lattice coincides with that in the zinc blende type lattice, if a relatively small deformation in the (111) direction takes place [21]. For this reason, the physical basis for the cubic approximation is based on a similarity between the (0001) axis in the wurtzite structure and the (111) direction in a cubic crystal [21].

The space group of the wurtzite structure is C_{6v}^4. The binding energy of the wurtzite structure is very close to that in the zinc-blende structure [20]. For this reason, GaN can crystallize in both structures.

It is known [20–23] that the spectrum of the valence band at point Γ results from the sixfold degenerate state $\Gamma_{15} \times D_{1/2}$. In the zinc-blende structure, level Γ_{15} is split due to the spin-orbit interaction, forming fourfold degenerate level Γ_8 of heavy (hh) and light (lh) holes, as well as double degenerate level Γ_7 of spin-split holes (sh), which belong to space group T_d^2. Being subjected to the hexagonal crystalline field and the spin-orbit interaction in a wurtzite crystal, level Γ_{15} get split, giving rise to the formation of three spin-degenerate levels, namely, Γ_9, upper Γ_7, and lower Γ_7 levels which are referred to as the band of heavy, light, and split holes, respectively, and belong to space group C_{6v}^4. The states in the conduction band in the vicinity of the Brillouin zone center are spin-degenerate, being characterized by a single effective mass in the case of cubic symmetry, and two effective masses in the case of hexagonal symmetry.

The Hamiltonian for the valence band of wurtzite, which takes the interaction of levels Γ_9, upper Γ_7, and lower Γ_7 into account, was obtained in the framework of the kp-method [22]. The derivation of the wurtzite Hamiltonian, which is based on the method of invariants and takes the influence of strains on the hole spectrum into account, was proposed in works [21, 24]. The transformation of the Hamiltonian written down in the $|1, m\rangle |1/2, s\rangle$ basis to the basis of angular momenta $3/2$ and $1/2$ with regard for the spin-orbit splitting was carried out in papers [23, 25]. The basis of angular momenta $3/2$ and $1/2$ is usually used for the Luttinger–Kohn six-dimensional Hamiltonian, when describing the zinc-blende structure. To use a unitary transformation for a block-diagonal form with two 3×3-blocks, which corresponds to the spin degeneration of states in the valence band, was proposed in works [23, 25, 26]. Just this approach was used in this work.

The structure of the paper is as follows. In Section 2, we introduce the well-known Hamiltonian of the valence band for both structures, zinc blende and wurtzite. The wave functions for the conduction and valence bands in an infinitely deep quantum well are presented. The matrix elements of the dipole moment and the light gain coefficient are given. In Section 3, original results on the strain dependences of the band structure, the matrix elements of the dipole moment, and the light gain spectrum are presented. Section 4 summarizes the results of our researches.

2. Theory

It is known [27] that the optical gain for a substance can be calculated using Fermi's golden rule

$$\alpha_0 = \frac{\pi e^2}{c \sqrt{\varepsilon} m_0 w \omega} \sum_{\sigma_c = \uparrow, \downarrow} \sum_{\sigma_v = +, -} \sum_{m, \alpha} \int k_t \, dk_t \times$$

$$\times \int \frac{d\phi}{2\pi} |\mathbf{e} \, M_{m\alpha}^{\sigma_c \sigma_v}(k_t)|^2 (f_m^c(k_t) - f_{\sigma_v \alpha}^v(k_t)) \times$$

$$\times \delta(E_{\sigma_v, m\alpha}^{cv}(k_t) - \hbar \omega), \tag{1}$$

where e is the electron charge, m_0 is the electron rest mass, c is the light velocity, ε is the dielectric permittivity of the substance, f_m^c and $f_{\sigma_v \alpha}^v$ are the Fermi–Dirac distribution functions for electrons in the conduction and valence bands, respectively, $\mathbf{e}$ is the unit vector of the vector potential of an electromagnetic wave, $E_{\sigma_v, m\alpha}^{cv}(k_t)$ is the energy gap between the conduction and valence bands, and $\hbar \omega$ is the optical energy.

We consider an electromagnetic wave which propagates in the quantum well plane. The gain coefficient, which defines the threshold laser ability, is proportional to the product of the substance gain coefficient α_0 and the optical confinement factor Γ. The latter is proportional to the well width and the number a of quantum

wells in multiplet quantum wells: $\alpha = \alpha_0 \Gamma a$. In the calculations, we suppose that $\Gamma = 0.01$ and $a = 1$.

Although charge carriers in each zone are in a strongly nonequilibrium state, the times of interband relaxation are much longer than those of intersubband relaxation. Hence, the Fermi–Dirac statistics can be used in calculations.

The quantity $M_{m\alpha}^{\sigma_c \sigma_v}(k_t) = \langle \Psi_{\alpha,k_t}^{v\sigma_v} | \hat{\mathbf{p}} | \Psi_{m,k_t}^{c\sigma_c} \rangle$ is the matrix element of the dipole moment for transitions between states in the conduction band, $\Psi_{m,k_t}^{c\sigma_c}(z)$, and the states in the valence one, $\Psi_{\alpha,k_t}^{v\sigma_v}(z)$, and $\hat{\mathbf{p}}$ is the momentum operator.

The initial state, which is supposed to belong to the conduction band, is described by the orbital Bloch function $|S\rangle$ and the spinor $|\sigma_c\rangle = |\uparrow\rangle, |\downarrow\rangle$ which corresponds to two directions of the electron spin. The wave function of the m-th conduction subband can be written down as

$$\Psi_{m,k_t}^{c\sigma_c}(\mathbf{r}) = \frac{e^{i\,k_t\,\rho_t}}{\sqrt{A}}\,\chi_m(z)|S\rangle|\sigma_c\rangle, \tag{2}$$

where A is the area of the quantum well in the plane xy, ρ_t is the two-dimensional vector in the same plane, $k_t = (k_x, k_y)$ is the wave vector in the quantum well plane, and $\chi_m(z)$ is the z-dependent part of the wave function envelope.

To symmetrize a p-like valence band, a similarity between p-like states and atomic p-wave functions is usually considered [20]. The p-states are known to be triply degenerate. We distinguish three states with the orbital angular momentum $l = 1$ and the eigenvalues m_l of its z-component – namely,

$$|1, \pm 1\rangle = (\mp|X\rangle - i\,|Y\rangle)/\sqrt{2}$$

and

$$|1, 0\rangle = |Z\rangle$$

– as well-known spherical harmonics. The eigenfunctions of a Hamiltonian, which includes the term of the spin-orbit interaction, are the eigenstates of the total angular momentum and its z-component. Therefore, the final state of the electron belongs to the valence band and can be determined by these eigenfunctions. The latter can be expressed as linear combinations of eigenfunctions of the orbital angular momentum and the spin, i.e. $|1, m_l\rangle|1/2, s\rangle$ (the projections $s = \pm 1/2$ are connected with two possible spin orientations) [28]:

$$\left|\Gamma_8(HH); \pm\frac{3}{2}\right\rangle = \frac{1}{\sqrt{2}}\,\left|\mp X - i\,Y, \pm\frac{1}{2}\right\rangle,$$

$$\left|\Gamma_8(LH); \pm\frac{1}{2}\right\rangle = \frac{1}{\sqrt{3}}\,\left(\left|\mp X - i\,Y, \mp\frac{1}{2}\right\rangle + \sqrt{2}\,\left|Z, \pm\frac{1}{2}\right\rangle\right),$$

$$\left|\Gamma_7(SH); \pm\frac{1}{2}\right\rangle = \frac{1}{\sqrt{3}}\,\left(\pm\sqrt{2}\,\left|\mp X - i\,Y, \mp\frac{1}{2}\right\rangle \mp \left|Z, \pm\frac{1}{2}\right\rangle\right). \tag{3}$$

The determination of "$(l = 1)$-like" states in GaN crystals with zinc-blend-like and wurtzite crystalline structures is based on the Hamiltonian [21, 22]

$$-H = \Lambda\,I + \Xi\,J_z^2 - \Delta_2\,J_z\,\sigma_z -$$

$$-\sqrt{2}\,\Delta_3\,(J_+\,\sigma_- + J_-\,\sigma_+) + \Pi\,J_+^2 + \Pi^*\,J_-^2 +$$

$$+2\,\Sigma\,[J_z J_+] + 2\,\Sigma^*\,[J_z J_-] + \Upsilon\,J_+ + \Upsilon^*\,J_-, \tag{4}$$

where

$$\Lambda = \Delta_1 + \Delta_2 + A_1\,k_z^2 + A_3\,k_t^2 + D_1\,\epsilon_{zz} + D_3\,\epsilon_t,$$

$$\Xi = -\Delta_1 + A_2\,k_z^2 + A_4\,k_t^2 + D_2\,\epsilon_{zz} + D_4\,\epsilon_t,$$

$$\Pi = A_5\,k_-^2 + D_5\,\epsilon_-,$$

$$\Sigma = A_6\,k_z\,k_- + D_6\,\epsilon_{-z},$$

$$\Upsilon = i\,\frac{\hbar^2\,\Re\,k_-}{2\,m_0},$$

$$k_\pm = k_x \pm i\,k_y,\ k_t^2 = k_x^2 + k_y^2,$$

$$J_\pm = \frac{1}{\sqrt{2}}\,(J_x \pm i\,J_y),\ 2\,[J_z\,J_\pm] = J_z\,J_\pm + J_\pm\,J_z,$$

$$\sigma_\pm = \frac{1}{2}\,(\sigma_x \pm i\,\sigma_y),$$

$$\epsilon_{\pm z} = \epsilon_{xz} \pm i\,\epsilon_{yz},\ \epsilon_\pm = \epsilon_{xx} - \epsilon_{yy} \pm 2\,i\,\epsilon_{xy},$$

and

$$\epsilon_t = \epsilon_{xx} + \epsilon_{yy}.$$

Strain effects are taken into account by adding the corresponding terms: $k_i k_j \to \epsilon_{ij}$, with the strain parameters

$D_1, \ldots, D_6$ in the corresponding positions of the effective mass parameters $A_1, \ldots, A_6$. Here, m_0 is the mass of a free electron; I is the identity matrix; J_x, J_y, and J_z are the components of the angular momentum operator; σ_x, σ_y, and σ_z are the Pauli matrices; $\Delta_1 \equiv \Delta_{cr}$ is the split energy induced by the hexagonal component of the crystalline field; $\Delta_{so}^z \equiv 3\Delta_2$ and $\Delta_{so}^t \equiv 3\Delta_3$ are the energies of the spin-orbit splitting in the z-direction and perpendicularly to it, respectively.

The term linear in the wave vector describes a loop of maxima in the valence band of a crystal with the wurtzite symmetry [29]. In the quasicubic GaN approximation, there is no term in the Hamiltonian which is linear in the wave vector [21].

The transformation of the Hamiltonian written down in the basis $|1, m_l\rangle|1/2, s\rangle$ to the basis of angular momenta $3/2$ and $1/2$ is carried out by means of Eq. (3) [23]. Choosing the unitary transformation in the same way as in the cubic case [23, 25],

$$|1, \pm\rangle = \frac{1}{\sqrt{2}}\left[|\tfrac{3}{2}, \tfrac{3}{2}\rangle\, e^{-3\,i\,\phi/2} \mp i\,|\tfrac{3}{2}, -\tfrac{3}{2}\rangle\, e^{3\,i\,\phi/2}\right],$$

$$|2, \pm\rangle = \frac{1}{\sqrt{2}}\left[\pm i\,|\tfrac{3}{2}, \tfrac{1}{2}\rangle\, e^{-i\,\phi/2} - |\tfrac{3}{2}, -\tfrac{1}{2}\rangle\, e^{i\,\phi/2}\right],$$

$$|3, \pm\rangle = \frac{1}{\sqrt{2}}\left[\pm i\,|\tfrac{1}{2}, \tfrac{1}{2}\rangle\, e^{-i\,\phi/2} + |\tfrac{1}{2}, -\tfrac{1}{2}\rangle\, e^{i\,\phi/2}\right], \quad (5)$$

where $\tan\phi = k_y/k_x$, we can transform the total 6×6-Hamiltonian into a block-diagonal one with the spin $\sigma_v = \pm$ [23]:

$$H = -\left\| \begin{array}{cc} H^+ & 0 \\ 0 & H^- \end{array} \right\|. \quad (6)$$

Here, $H^\pm$ for the biaxial strain defined above is expressed in the basis $[|1, \sigma_v\rangle, |2, \sigma_v\rangle, |3, \sigma_v\rangle]$ as follows:

$$H^\pm =$$

$$= \left\| \begin{array}{ccc} P + Q & R \mp i\,S & \sqrt{2}\,R \pm \frac{i}{\sqrt{2}}\,S \\ R \pm i\,S & P - Q & \sqrt{2}\,Q \pm i\,\sqrt{\frac{3}{2}}\,S \\ \sqrt{2}\,R \mp \frac{i}{\sqrt{2}}\,S & \sqrt{2}\,Q \mp i\,\sqrt{\frac{3}{2}}\,S & P + \Delta_{so} \end{array} \right\|,$$

$$(7)$$

where

$$P = \frac{1}{3}\Delta_{cr} + \alpha_1 k_z^2 + \alpha_2 k_t^2 + d_1 \epsilon_{zz} + d_2(\epsilon_{xx} + \epsilon_{yy}),$$

$$Q = -\frac{1}{3}\Delta_{cr} - 2\alpha_3 k_z^2 + \alpha_4 k_t^2 - 2d_3 \epsilon_{zz} + d_4(\epsilon_{xx} + \epsilon_{yy}),$$

$$R = \sqrt{3}\alpha_5 k_t^2,$$

$$S = 2\sqrt{3}\alpha_6 k_z k_t,$$

and

$$k_t^2 = k_x^2 + k_y^2.$$

The relations between the parameters introduced here and the parameters of the Hamiltonian in the basis $|1, m_l\rangle|1/2, s\rangle$ can be written down in the form

$$\alpha_1 = A_1 + \frac{2}{3}A_2, \ \ \alpha_2 = A_3 + \frac{2}{3}A_4, \ \ \alpha_3 = -\frac{1}{6}A_2,$$

$$\alpha_4 = \frac{1}{3}A_4, \ \ \alpha_5 = -\frac{1}{3}A_5, \ \ \alpha_6 = -\frac{1}{3\sqrt{2}}A_6,$$

$$\Delta_{cr} = \Delta_1, \ \ \Delta_{so} = 3\Delta_2 = 3\Delta_3. \quad (8)$$

In a similar manner, the parameters of the deformation potential can be expressed as

$$d_1 = D_1 + \frac{2}{3}D_2, \ \ d_2 = D_3 + \frac{2}{3}D_4,$$

$$d_3 = -\frac{1}{6}D_2, \ \ d_4 = \frac{1}{3}D_4. \quad (9)$$

The parameters A_1 to A_6 are connected with the Luttinger-like parameters [23]:

$$-A_1 = \gamma_{1z} + 4\,\gamma_{3z}, \ \ -A_2 = \gamma_{1t} - 2\,\gamma_{3t}, \ \ A_3 = 6\,\gamma_{3z}$$

$$-A_4 = 3\,\gamma_{3t}, \ \ A_5 = \gamma_{2t} + 2\,\gamma_{3t}, \ \ A_6 = \sqrt{2}\,(2\,\gamma_{2z} + \gamma_{3z}). \quad (10)$$

In a similar manner, the relations for the parameters of the deformation potential can be expressed as

$$-D_1 = \delta_{1z} + 4\,\delta_{3z}, \ \ -D_2 = \delta_{1t} - 2\,\delta_{3t}, \ \ D_3 = 6\,\delta_{3z}$$

$$-D_4 = 3\,\delta_{3t}, \ \ D_5 = \delta_{2t} + 2\,\delta_{3t}, \ \ D_6 = \sqrt{2}\,(2\,\delta_{2z} + \delta_{3z}). \quad (11)$$

The relations between the Luttinger-like parameters, the Luttinger parameters γ_1, γ_2, and γ_3, and the deformation potentials a_v, b, and d in a cubic crystal are simple [23]:

$$\gamma_{1z} = \gamma_{1t} \to \gamma_1, \; \gamma_{2z} = \gamma_{2t} \to \gamma_2, \gamma_{3z} = \gamma_{3t} \to \gamma_3, \quad (12)$$

$$\delta_{1z} = \delta_{1t} \to -a_v, \; \delta_{2z} = \delta_{2t} \to -b/2,$$

$$\delta_{3z} = \delta_{3t} \to -d/2\sqrt{3}. \quad (13)$$

In both cubic and hexagonal substances, the vertex of the sixfold degenerate valence band originates from atomic p^3-orbitals, which correspond to the vector representation for Γ_{15} and are split due to either the spin-orbit interaction or the hexagonal crystal field [20, 21]. We calculate the matrix elements of the dipole moment making use of the vector representation for Bloch functions. We introduce the Bloch function written down as a vector in the three-dimensional Bloch space:

$$|\alpha\,\sigma_v\,k_t\rangle = \left\| \begin{matrix} \phi_\alpha^{(1)}(z, k_t) \\ \phi_\alpha^{(2)}(z, k_t) \\ \phi_\alpha^{(3)}(z, k_t) \end{matrix} \right\| \left\| \begin{matrix} |1, \sigma_v\rangle \\ |2, \sigma_v\rangle \\ |3, \sigma_v\rangle \end{matrix} \right., \quad (14)$$

where

$$\phi_\alpha^{(j)} = \sum_{i=1}^{n} V_{k_t}^{(j)}[i, \alpha]\, \chi_i(z). \quad (15)$$

The Bloch vector of the α-type for a hole with the spin $\sigma_v = \pm$ and the wave vector k_t is determined by three coordinates $[V_{k_t}^{(1)}[n, \alpha], V_{k_t}^{(2)}[n, \alpha], V_{k_t}^{(3)}[n, \alpha]]$ in the basis $[|1, \sigma_v\rangle, |2, \sigma_v\rangle, |3, \sigma_v\rangle]$. The z-dependent part of the envelopes of quantum well eigenfunctions can be determined in the case of boundary conditions for an infinitely deep quantum well, $\chi_n(z = -w/2) = \chi_n(z = w/2) = 0$, as

$$\chi_n(z) = \sqrt{\frac{2}{w}} \sin\left(\pi\, n\, \left(\frac{z}{w} + \frac{1}{2}\right)\right), \quad (16)$$

where n is a natural number. The hole wave function can be written down as

$$\Psi_{\alpha, k_t}^{v\sigma_v}(\mathbf{r}) = \frac{e^{i\, k_t\, \rho_t}}{\sqrt{A}}\, |\alpha\,\sigma_v\,k_t\rangle. \quad (17)$$

The valence band structure $E_\alpha^{\sigma_v}(k_t)$ can be determined by solving the equation

$$\sum_{j=1}^{3} (H_{ij}^{\sigma_v}(k_z = -i\,\frac{\partial}{\partial z}) + \delta_{ij} E_\alpha^{\sigma_v}(k_t)) \times$$

$$\times \phi_\alpha^{(j)\sigma_v}(z, k_t) = 0, \quad (18)$$

where $i = 1, 2, 3$.

On the basis of the symmetry properties of Bloch functions, a conclusion can be drawn that only the following nonzero matrix elements between basic functions exist [23, 28]:

$$\langle\, S|\hat{p}_z|1, 0\rangle = P_z,$$

$$\langle\, S|\hat{p}_+|1, -1\rangle = -\langle\, S|\hat{p}_-|1, 1\rangle = \sqrt{2}\, P_\perp, \quad (19)$$

where $\hat{p}_\pm = \hat{p}_x \pm i\,\hat{p}_y$. Two matrix elements of the dipole moment are determined as $P_\perp \equiv \langle\, S|\hat{p}_x|X\rangle$ and $P_z \equiv \langle\, S|\hat{p}_z|Z\rangle$.

The matrix elements of the dipole moment for the x- or y-polarization ($\mathbf{e} \perp z$) can be determined as follows [31]:

$$|e_x M_{m\,\alpha}^{\uparrow\,+}(k_t)|^2 = \frac{|\langle\, S|\hat{p}_x|X\rangle|^2}{4} \times$$

$$\times \left(|\langle\chi_m|\phi_\alpha^{(1)}\rangle|^2 + \frac{1}{3}\,|\langle\chi_m|\phi_\alpha^{(2)}\rangle|^2 + \right.$$

$$+ \frac{2}{3}\,|\langle\chi_m|\phi_\alpha^{(3)}\rangle|^2 + \frac{\sqrt{8}}{3}\,\langle\chi_m|\phi_\alpha^{(2)}\rangle\,\langle\chi_m|\phi_\alpha^{(3)}\rangle +$$

$$+ \frac{2}{\sqrt{3}}\,\cos 2\phi\,\langle\chi_m|\phi_\alpha^{(1)}\rangle\,\langle\chi_m|\phi_\alpha^{(2)}\rangle +$$

$$\left. + \sqrt{\frac{8}{3}}\,\cos 2\phi\,\langle\chi_m|\phi_\alpha^{(1)}\rangle\,\langle\chi_m|\phi_\alpha^{(3)}\rangle \right). \quad (20)$$

The matrix elements for the z-polarization ($\mathbf{e} \parallel z$) can be given as

$$|e_z M_{m\,\alpha}^{\uparrow\,+}(k_t)|^2 = \frac{|\langle\, S|\hat{p}_z|Z\rangle|^2}{3} \left(|\langle\chi_m|\phi_\alpha^{(2)}\rangle|^2 + \right.$$

$$\left. + \frac{1}{2}\,|\langle\chi_m|\phi_\alpha^{(3)}\rangle|^2 - \sqrt{2}\,\langle\chi_m|\phi_\alpha^{(2)}\rangle\,\langle\chi_m|\phi_\alpha^{(3)}\rangle \right). \quad (21)$$

Numerical values of the constants $|P_{z,\perp}|^2$ can be found [23] in the framework of the kp-theory –

$$\frac{m_0}{m_{z,x}^{(c)}} = 1 + \frac{2}{m_0} \Sigma_{j\neq c} \frac{|\langle c|\hat{p}_{z,x}|j\rangle|^2}{E_c^0 - E_j^0} \quad (22)$$
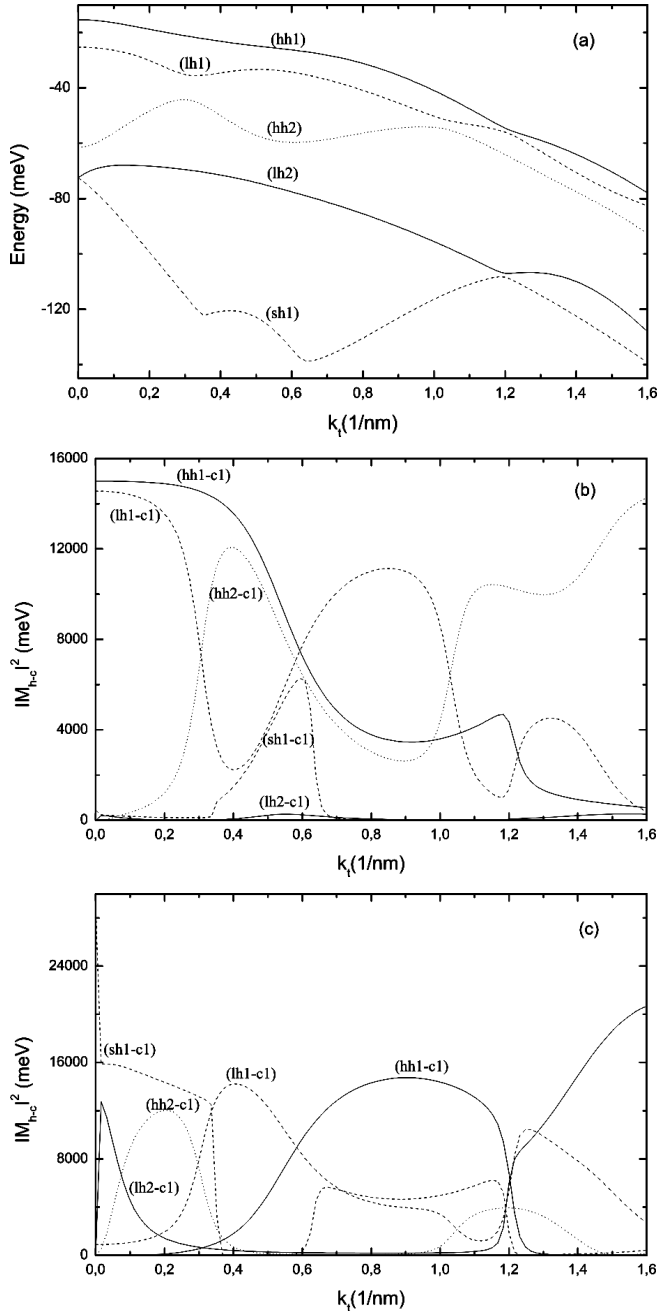
Fig. 1. (*a*) valence band structure; matrix elements of the electric dipole moment for (*b*) *x*- or *y*- and (*c*) *z*-polarizations for an undeformed thin GaN film

– by the formula

$$\frac{2\left|P_{z,\perp}\right|^2}{m_0} \simeq E_g\left(\frac{m_0}{m_{z,\perp}^{(c)}} - 1\right),\qquad(23)$$

making use of experimentally measured effective masses $m_{z,\perp}^{(c)}$. Here, we use the same numerical values for the

effective mass, the energy of spin-orbit splitting, and the deformation potential parameters as in works [23, 30, 31].

3. Results and Their Discussion

We consider a pseudomorphically deformed $GaN/Al_{0.14}Ga_{0.86}N$ quantum well 6 nm in width and assume a rectangular potential shape for it. The results of numerical calculations of the valence band spectrum and the dependences of matrix elements on the wave vector $k_t = (k_x, k_y)$, which lies in the quantum well plane, are presented in Figs. 1 to 3. Here, for all structures, two the highest hole subbands are the subbands of heavy and light holes.

In order to elucidate the role of biaxial compressive-tensile strains, we consider an undeformed thin GaN film. In Fig. 1, the corresponding valence band structure and the k-dependences of matrix elements are demonstrated. Figure 1,*a* shows that each band contains a mixture of heavy, light, and spin-orbit-split hole states.

It is known that the p-like sixfold spin-degenerate valence band in cubic crystals becomes split at point Γ into fourfold degenerate level Γ_8 and double degenerate level Γ_7 due to the spin-orbit interaction. The magnitude of this splitting is the energy of spin-orbit splitting, which is determined by the matrix element of the Hamiltonian of the spin-orbit interaction between atomic orbitals. Usually, it is referred to as the spin-orbit splitting width. Degeneration originates from cubic symmetry and can be obtained from Γ_8-representation. In the case where the quantum well is grown up along the (001) direction, the crystal symmetry decreases to the tetragonal one [32]. This means the elimination of Γ_8-state degeneration, as is shown in Fig. 1,*a*.

In Fig. 2, the valence band structure and the k-dependences for the matrix elements of a quantum well at a biaxial compressive strain are depicted. The strain components are $\epsilon_{xx} = -0.0041$ and $\epsilon_{zz} = 0.0047$. This strain corresponds to the 14% aluminum content. Such an Al content in the $Al_xGa_{1-x}N$ material structure gives rise a mismatch between its lattice constants and those of GaN. From Fig. 2,*a*, one can see that a compressive strain lowers valence bands with respect to their positions in a thin film. Such a behavior agrees with the results of calculations dealing with the deformation effects on the valence band structure in (0001) wurtzite GaN quantum wells which are used for nitride-based devices on sapphire substrates [33].

We consider optical transitions between the following initial and final states: with the angular momentum $J = 3/2$ and the magnetic quantum numbers
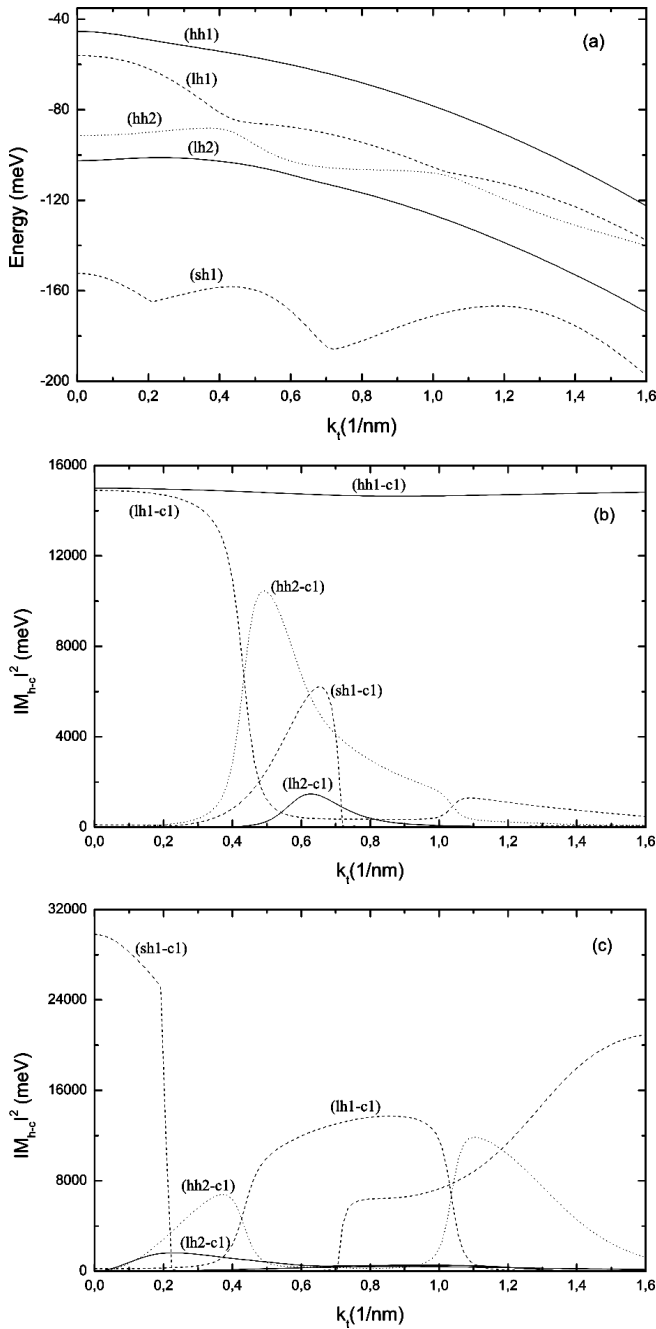
Fig. 2. The same as in Fig. 1, but for a GaN/AlGaN quantum well at the biaxial compressive strain $\epsilon_{xx} = -0.41\%$

Fig. 3. The same as in Fig. 1, but for a GaN/AlGaN quantum well at the biaxial tensile strain $\epsilon_{xx} = 0.41\%$

$m_j = \pm 3/2, \pm 1/2$ in the valence band, with $J = 1/2$ and $m_j = \pm 1/2$ in the same band, and with $J = 1/2$ and $m_j = \pm 1/2$ in the conduction band. The transitions from the valence band states with $m_j = \pm 1/2$ satisfy the selection rules $\Delta m = 0$ and $\Delta m = \pm 1$; therefore, they have both x- (or y-) and z-oriented light polarization.
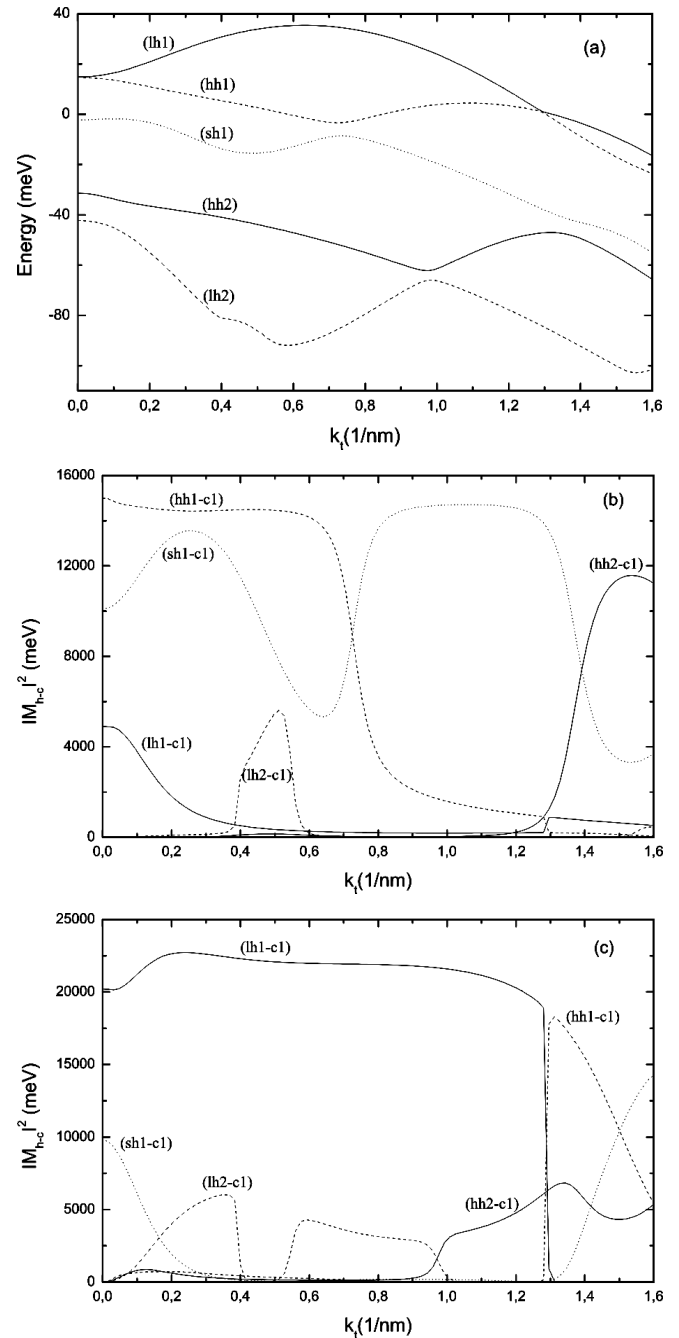
The transitions from the states $m_j = \pm 3/2$ of the valence band satisfy the selection rules $\Delta m = \pm 1$; hence, they are only x- or y-polarized [28].

At a compressive deformation, the growth of aluminum content is accompanied by the growth of splitting width between the heavy- and light-hole bands and the
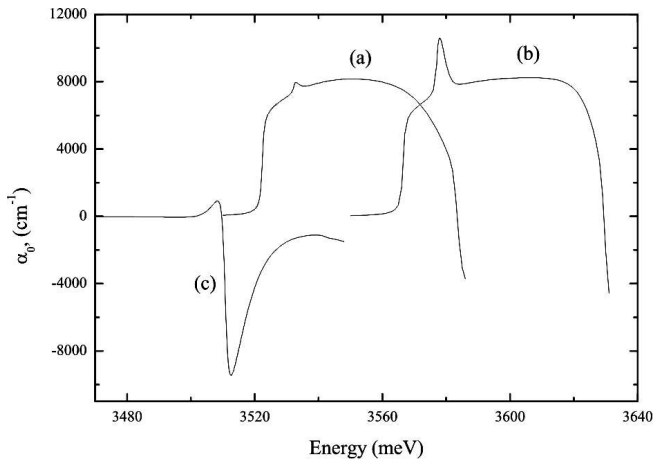
Fig. 4. Light gain factor of a GaN/AlGaN quantum well for: (a) x- or y-polarization of undeformed quantum well, (b) x- or y-polarization at the biaxial compressive strain $\epsilon_{xx} = -0.41\%$, (c) z-polarization at the biaxial tensile strain $\epsilon_{xx} = 0.41\%$

reduction of the valence band mixing effect. Let us consider transitions from the heavy-hole band. Figures 1 and 2 evidently illustrate that the contribution of x (or y) light polarization is larger, if one moves from an undeformed thin film to a deformed heterostructure, in which $\epsilon_{xx} = -0.0041$. Hence, in the case of a quantum well subjected to a biaxial compressive strain, the matrix elements have a strict x (or y) light polarization. Such a behavior agrees with the results of calculations [21,34,35] of the matrix elements of the dipole moment in crystals with the wurtzite symmetry and the corresponding quantum-well structures, in which the considered transitions are allowed for x (or y) light polarization, while they are forbidden for the z one.

In Fig. 3, we exhibit the valence band structure and the k-dependences of matrix elements for a quantum well at a biaxial tensile strain. The strain components are $\epsilon_{xx} = 0.0041$ and $\epsilon_{zz} = -0.0047$. Figure 3,a demonstrates that the tensile deformation brings about a strong modification of the hole effective mass and a reduction of the splitting width, since the light-hole band shifts upwards to the top of the heavy-hole band. The first phenomenon results in the emergence of a large negative mass at the center of the Brillouin zone, whereas the second one is responsible for the appearance of "random" double degeneration of spin-degenerate states of heavy and light holes at the center of the Brillouin zone. We show that the fourfold degeneration of states in the valence band at the center of the Brillouin zone of the (001) zinc-blende GaN quantum well: first, the states of heavy and light holes become spin-degenerate, and,

afterwards, there emerges the additional "random" double degeneration under the action of a tensile strain. In general, the degeneration is the reason for the density-of-states growth. If the tensile strain grows further, the light-hole band can shift above the heavy-hole one, which means the elimination of the fourfold degeneration of states in the valence band. Therefore, if $\epsilon_{xx} > 0.0041$, the light-hole band becomes the highest among the quantized hole subbands. It is expected that the density of states would change under the action of a biaxial tensile strain. Such a behavior qualitatively agrees with the results of researches of the influence of internal strain effects on the valence band structure of $Si_{1-x}Ge_x$ [36].

In zinc-blende GaN, the light-hole band states include both $|X \pm iY\rangle$ and $|Z\rangle$ ones. A comparison between Figs. 1 and 3 shows the growing presence of state $|Z\rangle$ in the light-hole band, if we move from an undeformed thin film to a deformed heterostructure, where $\epsilon_{xx} = 0.0041$. Therefore, a greater contribution of state $|Z\rangle$ is observed in the light-hole band in the deformed heterostructure than that in a thin film. Hence, in a deformed quantum well with $\epsilon_{xx} > 0.0041$, the contribution of the $|Z\rangle$-function, which generates a strong matrix element for z-polarization of light, dominates in the states belonging to the highest light-hole subband.

Although biaxial compression-tensile deformations were studied, only the GaN quantum well with the zinc blende type structure reveals a spectral section with a negative effective mass and a strong modification of matrix elements for z-polarization of light at stretching. The density of states, the inverse level population by carriers, the matrix elements, and the light gain spectrum are changed specifically, when a negative effective mass emerges at the center of the Brillouin zone.

Our understanding of the effects induced by internal deformations owing to a lattice mismatch is crucial for improving the laser characteristics and the optimal design of a device.

In Fig. 4, the dependences of the light gain factor on the energy in the quantum well with a charge carrier concentration of 4×10^{12} cm^{-2} are shown for such a light polarization that the corresponding optical transitions are allowed by selection rules, i.e. by the calculated matrix elements. The temperature is 4.4 K. As soon as we obtain an inverse interband population, the light intensity becomes enhanced. The growth of the electron-hole concentration makes the effective electron-hole recombination in the heterostructure possible, which provides the high optical gain factor of a laser. It is shown that, under the action of a biaxial compression, the displacements of the valence and conduction bands give rise to

a blue shift of the gain spectrum with respect to the absorption edge of an undeformed quantum well, as is shown in Fig. 4. In Fig. 4,*b*, we illustrate a possibility of stimulated emission in the wavelength range between 347.5 and 340.8 nm in a zinc-blende GaN/Al$_{0.14}$Ga$_{0.86}$N quantum well under the action of a compressive strain. The peak of the gain spectrum was determined to be at a wavelength of 345.4 nm. Semiconductor laser diodes and light emitting diodes can emit ultra-violet light owing to a wide-band-gap nature of the GaN substance. Here, we suppose the energy gap width to be 3.5 eV. In Fig. 4,*b*, the structure of the gain spectrum is well pronounced due to the contributions of optical transitions from both heavy- and light-hole subbands. As the temperature grows, the structure of the gain spectrum gets smeared.

The effective mass was found to change drastically at a tensile deformation. The emergence of a negative effective mass at the center of the Brillouin zone allows the gain factor sign to change, as is shown in Fig. 4. It can be explained by the appearance of a loop with the radius $k_t \approx 0.6$ nm^{-1} in the valence band structure of the quantum well of zinc-blende GaN under the action of a tensile strain. Effects of the extremum loop, which originate from a term linear in the wave vector in the wurtzite Hamiltonian, are known from works [29]. However, in our research, the extremum loop arose due to the entanglement of the heavy- and light-hole subbands. As soon as the spectral range with a negative effective mass emerges, the holes are localized at the loop of valence band maxima. As a result, the optical transitions near the absorption edge are accompanied with high absorption of light in the ultra-violet range, in the interval from 352.4 to 349.5 nm, suppressing the laser effect. At a tensile deformation, the displacements of the valence and conduction bands give rise to a red shift of the absorption spectrum with respect to the absorption edge of the undeformed quantum well.

In the zinc-blende and wurtzite crystals, every atom is surrounded by four closest neighbors forming a perfect tetrahedron. The valence electrons of such a crystalline structure form hybridized sp^3-orbitals [20]. Those sp^3-hybridizations are well-known for bonds in a methane molecule. It is of interest to consider the analogy that exists between the dependence of matrix elements on the strain and the influence of deformation effects on the behavior of angles between bonds in a tetrahedron. It is known [37] that, in the case of a biaxial tensile strain, the tetrahedron bonds become squeezed along the *c*-axis, so that the distances from the Ga-N layers to the planar

structure become shorter, and the angles between bonds change. This stimulates the dehybridization of ideal sp^3-hybrids into sp^2- and p_z-orbitals. In such a manner, the quantum-mechanical problem of dehybridization of sp^3-hybrids into sp^2- and p_z-orbitals explains the tendency for the state $|Z\rangle$ to grow in the light-hole subband at a tensile deformation, which generates the matrix element for the *z*-polarization, as is shown in Fig. 3,*c*.

Hence, one can see in Fig. 4 that the variations of both the sign and the polarization of the gain coefficient in the heterostructure are distinctly pronounced.

4. Conclusions

We studied the influence of strain effects on the valence band structure, the interband matrix elements, and the light gain spectrum in a pseudomorphically deformed zinc-blend GaN quantum well. With this purpose in view, we used the 3×3-Hamiltonian to calculate the spectrum of the valence band in the heterostructure. A detailed analysis for the dependence of the hole spectrum, the matrix elements, and the light gain spectrum on the strain emerging due to the lattice mismatch in the heterostructure has been made. The analysis of the band structure of a quantum well at a compressive deformation testifies to a reduction of the valence band energy. If the quantum well is subjected to squeezing, the matrix elements for the transitions from the first hole band have a strict light polarization, with the polarization vector laying in the quantum well plane. On the other hand, at stretching, those matrix elements are strictly polarized in the direction perpendicular to the quantum well plane. A tensile strain is accompanied by the emergence of a large effective mass at the center of the Brillouin zone and a considerable modification of matrix elements. At the center of the Brillouin zone, there appears the "random" double spin-degeneration of heavy-and light-hole states. For a tensile deformation of the heterostructure, the growth of the state $|Z\rangle$ in the light-hole band was found. It has to induce a considerable polarization of the matrix element in the direction perpendicular to the quantum well plane. A loop of valence band maxima with a confined radius was found in the heterostructure subjected to a tensile strain. The paper demonstrates the importance of the loop of the valence band extremum. At a compressive deformation, holes are localized at the vertices of valence subbands, and, in the case of a tensile deformation, at the cyclic loop of valence subband maxima. The laser effect was shown to be suppressed in the GaN quantum well at a tensile deforma-

tion, whereas the stimulated emission in the ultra-violet region is distinctly pronounced at a compressive one. Although the extremum loop effects in wurtzite crystals have been studied earlier [29], the suppression of the laser effect was not mentioned in publications. In general, the internal deformation effects can be marked as those playing a considerable role in the study of optical properties of heterostructures. It should be noted that our research does not take into account polarization effects, which are very important in such structures.

1. S. Nakamura and G. Fasol, *The Blue Laser Diode* (Springer, Berlin, 1997); R.L. Aggarwal, P.A. Maki, Z.-L. Liau, and I. Melngailis, J. Appl. Phys. **79**, 2148 (1996); S. Nakamura, M. Senoh, S. Nagahama, N. Iwasa, T. Yamada, T. Matsushita, H. Kiyoku, and Y. Sugimoto, Jpn. J. Appl. Phys. **35**, L74 (1996); S. Nakamura, J. Vac. Sci. Technol. A **13**, 705 (1995).

2. N. Savage, Nature Photonics **1**, 83 (2007).

3. M. Asif Khan *et al.*, J. Appl. Phys. **76**, 1161 (2000).

4. M. Iwaya, S. Takanami, A. Miyazaki, Y. Wanatabe, S. Kamiyama, H. Amano, and I. Akasaki, Phys. Status Solidi A **188**, 117 (2001).

5. G. Kipshidze, V. Kuryatkov, B. Borisov, M. Holtz, S. Nikishin, and H. Temkin, J. Appl. Phys. **93**, 1363 (2003).

6. J.P. Zhang *et al.*, Appl. Phys. Lett. **81**, 4910 (2002).

7. V. Adivarahan, S. Wu, J. P. Zhang, R. A. Chitnis, M. Shatalov, V. Mandavilli, R. Gaska, and M.A. Khan, Appl. Phys. Lett. **84**, 4762 (2004).

8. A. Khan, K. Balakrishnan, and T. Katona, Nature Photonics **2**, 77 (2008).

9. S. Nagahama, T. Yanamoto, M. Sano, and T. Mukai, Jpn. J. Appl. Phys. **40**, L788 (2001).

10. S. Nagahama, T. Yanamoto, M. Sano, and T. Mukai, Jpn. J. Appl. Phys. **41**, 5 (2002).

11. M. Kneissl, D. Treat, M. Teepe, N. Miyashita, and N.M. Johnson, Appl. Phys. Lett. **82**, 2386 (2003).

12. M. Kneissl, D. Treat, M. Teepe, N. Miyashita, and N.M. Johnson, Appl. Phys. Lett. **82**, 4441 (2003).

13. S. Masui, Y. Matsuyama, T. Yanamoto, T. Kozaki, S. Nagahama, and T. Mukai, Jpn. J. Appl. Phys. **42**, L1318 (2003).

14. K. Iida *et al.*, Jpn. J. Appl. Phys. **43**, L499 (2004).

15. T. Takano, Y. Narita, A. Horiuchi, and H. Kawanishi, Appl. Phys. Lett. **84**, 3567 (2004).

16. H. Markoç, S. Strite, G.B. Gao, M.E. Lin, B. Sverdlov, and M. Burns, J. Appl. Phys. **76**, 1363 (1994).

17. W.G. Perry, T. Zheleva, M.D. Bremser, R.F. Davies, W. Shan, and J.J. Song, J. Electron. Mater. **26**, 224 (1997).

18. S. C. Jain, M. Willander, J. Narayan, and R. Van Overstraeten, J. Appl. Phys. **87**, 965 (2000).

19. *Semiconductors*, edited by O. Madelung (Springer, Berlin, 1991); W. Shan, T.J. Schmidt, X.H. Yang, S.J. Hwang, J.J. Song, and B. Goldenberg, Appl. Phys. Lett. **66**, 985 (1995).

20. P.Y. Yu and M. Cardona, *Fundamentals of Semiconductors* (Springer, Berlin, 1996).

21. G.L. Bir and G.E. Pikus, *Symmetry and Strain-Induced Effects in Semiconductors* (Wiley, New York, 1974).

22. E.I. Rashba, Fiz. Tverd. Tela **1**, 407 (1959); E.I. Rashba and V.I. Sheka, Fiz. Tverd. Tela **1**, 162 (1959); G.E. Pikus, Zh. Èksp. Teor. Fiz. **41**, 1258 (1961); Sov. Phys. JETP **14**, 898 (1962).

23. Yu.M. Sirenko, J.-B. Jeon, K.W. Kim, M.A. Littlejohn, and M.A. Stroscio, Phys. Rev. B **53**, 1997 (1996).

24. J.M. Luttinger, Phys. Rev. **102**, 1030 (1956).

25. S.Y.-P. Chao and S.L. Chuang, Phys. Rev. B **46**, 4110 (1992).

26. S.L. Chuang and C.S. Chang, Phys. Rev. B **54**, 2491 (1996).

27. V.V. Mitin, V.A. Kochelap, and M.A. Stroscio, *Quantum Heterostructures* (Cambridge University Press, New York, 1999).

28. L.D. Landau and E.M. Lifshitz, *Quantum Mechanics. Non-Relativistic Theory* (Pergamon, New York, 1977).

29. R.C. Casella, Phys. Rev. Lett. **5**, 371 (1960); E.I. Rashba, Fiz. Tverd. Tela **2**, 1224 (1960); G.D. Mahan and J.J. Hopfield, Phys. Rev. **135A**, 428 (1964); L.C. Voon *et al.*, Phys. Rev. B **53**, 10703 (1996).

30. W.J. Fan, M.F. Li, T.C. Chong, and J.B. Xia, J. Appl. Phys. **79**, 188 (1996).

31. C.-H. Kim and B.-H. Han, Solid State Commun. **106**, 127 (1998).

32. M. Suzuki and T. Uenoyama, Appl. Phys. Lett. **69**, 3378 (1996).

33. Yu.M. Sirenko, J.-B. Jeon, K.W. Kim, M.A. Littlejohn, and M.A. Stroscio, Appl. Phys. Lett. **69**, 2504 (1996).

34. R.C. Casella, Phys. Rev. **114**, 1514 (1959).

35. S.L. Chuang, J. Quant. Electr. **32**, 1791 (1996).

36. T. Yamada and D.K. Ferry, Solid State Electr. **38**, 881 (1995).

37. J.-M. Wagner and F. Bechstedt, Phys. Rev. B **66**, 115202 (2002).

ВАЛЕНТНА ЗОННА СТРУКТУРА, ОПТИЧНІ
ПЕРЕХОДИ І СПЕКТР ПІДСИЛЕННЯ СВІТЛА
В ПСЕВДОМОРФІЧНО ЗДЕФОРМОВАНІЙ
КВАНТОВІЙ ЯМІ GaN З ҐРАТКОЮ
ЦИНКОВОЇ ОБМАНКИ

Л. О. Локоть

Р е з ю м е

В статті вивчено вплив ефектів деформації на спектр валентної зони, міжзонні матричні елементи і спектр підсилення світла в квантовій ямі GaN з ґраткою цинкової обманки. В рамках теорії ефективної маси розв'язується рівняння Шредінгера для валентної зони, яка описується гамільтоніаном розмірністю 3×3. Наведено результати для квантової ями $GaN/Al_{0,14}Ga_{0,86}N$. Знайдено, що при двовісній деформації стиску, матричні елементи оптичних переходів з підзони важких дірок мають строгу поляризацію світла з вектором, який лежить в площині квантової ями. Показано, що походження великої негативної маси і сильна модифікація матричних елементів електричного дипольного моменту пов'язані з ефектами двовісної деформації розтягу. Знайдено "випадкове" двократне виродження вироджених за спіном станів важких і легких дірок в центрі зони Бріллюена. Знайдено великий матричний елемент електричного дипольного моменту для поляризації світла в напрямку, перпендикулярному до площини квантової ями. Показано, що двовісна деформація є причиною дуже значних змін в спектрі підсилення гетероструктур. Показано, що лазерний ефект подавлений під час виникнення петлі максимумів валентної зони в гетероструктурі при деформації розтягу, натомість при деформації стиску стимульовані оптичні переходи яскраво виражені. Наші результати свідчать про те, що внутрішні деформаційні ефекти важливі у вивченні оптичних властивостей GaN і відповідних гетероструктур.